

PUBLISHED VERSION

Marie-Therese Haider, Ingunn Holen, T. Neil Dear, Keith Hunter, Hannah K. Brown
Modifying the osteoblastic niche with zoledronic acid in vivo - potential implications for breast cancer bone metastasis
Bone, 2014; 66:240-250

© 2014 The Authors. Published by Elsevier Ltd. This is an open access under the CC BY-NC-SA license (<http://creativecommons.org/licenses/by/3.0/>).

Originally published at:
<http://doi.org/10.1016/j.bone.2014.06.023>

PERMISSIONS

<http://creativecommons.org/licenses/by-nc-sa/3.0/>



Attribution-NonCommercial-ShareAlike 3.0 Unported (CC BY-NC-SA 3.0)

This is a human-readable summary of (and not a substitute for) the [license](#).

[Disclaimer](#)

You are free to:

Share — copy and redistribute the material in any medium or format

Adapt — remix, transform, and build upon the material

The licensor cannot revoke these freedoms as long as you follow the license terms.

Under the following terms:



Attribution — You must give **appropriate credit**, provide a link to the license, and **indicate if changes were made**. You may do so in any reasonable manner, but not in any way that suggests the licensor endorses you or your use.



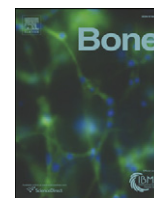
NonCommercial — You may not use the material for **commercial purposes**.



ShareAlike — If you remix, transform, or build upon the material, you must distribute your contributions under the **same license** as the original.

No additional restrictions — You may not apply legal terms or **technological measures** that legally restrict others from doing anything the license permits.

<http://hdl.handle.net/2440/90935>



Original Full Length Article

Modifying the osteoblastic niche with zoledronic acid *in vivo*—Potential implications for breast cancer bone metastasis



Marie-Therese Haider^a, Ingunn Holen^a, T. Neil Dear^b, Keith Hunter^c, Hannah K. Brown^{d,*}

^a CR-UK/YCR Cancer Research Centre, University of Sheffield, Sheffield, UK

^b South Australian Health and Medical Research Institute, Adelaide, South Australia, Australia

^c School of Clinical Dentistry, University of Sheffield, Sheffield, UK

^d The Mellanby Centre for Bone Research, Department of Human Metabolism, The University of Sheffield, Sheffield, S10 2RX, UK

ARTICLE INFO

Article history:

Received 21 March 2014

Revised 12 June 2014

Accepted 18 June 2014

Available online 24 June 2014

Edited by: J. Aubin

Keywords:

Metastatic niche

Osteoblast

Osteoclast

Breast cancer

Homing

ABSTRACT

Introduction: Bone metastasis is the most common complication of advanced breast cancer. The associated cancer-induced bone disease is treated with bone-sparing agents like zoledronic acid. Clinical trials have shown that zoledronic acid also reduces breast cancer recurrence in bone; potentially by modifying the bone microenvironment surrounding disseminated tumour cells. We have characterised the early effects of zoledronic acid on key cell types of the metastatic niche *in vivo*, and investigated how these modify the location of breast tumour cells homing to bone.

Methods: Female mice were treated with a single, clinically achievable dose of zoledronic acid (100 µg/kg) or PBS. Bone integrity, osteoclast and osteoblast activity and number/mm trabecular bone on 1, 3, 5 and 10 days after treatment were assessed using µCT, ELISA (TRAP, PINP) and bone histomorphometry, respectively. The effect of zoledronic acid on osteoblasts was validated in genetically engineered mice with GFP-positive osteoblastic cells. The effects on growth plate cartilage were visualised by toluidine blue staining. For tumour studies, mice were injected *i.c.* with DID-labelled MDA-MB-231-NW1-luc2 breast cancer cells 5 days after zoledronic acid treatment, followed by assessment of tumour cell homing to bone and soft tissues by multiphoton microscopy, flow cytometry and *ex vivo* cultures.

Results: As early as 3 days after treatment, animals receiving zoledronic acid had significantly increased trabecular bone volume vs. control. This rapid bone effect was reflected in a significant reduction in osteoclast and osteoblast number/mm trabecular bone and reduced bone marker serum levels (day 3–5). These results were confirmed in mice expressing GFP in osteoblastic lineage cells. Pre-treatment with zoledronic acid caused accumulation of an extra-cellular matrix in the growth plate associated with a trend towards preferential [1] homing of tumour cells to osteoblast-rich areas of bone, but without affecting the total number of tumour cells. The number of circulating tumour cells was reduced in ZOL treated animals.

Conclusion: A single dose of zoledronic acid caused significant changes in the bone area suggested to contain the metastatic niche. Tumour cells arriving in this modified bone microenvironment appeared to preferentially locate to osteoblast-rich areas, supporting that osteoblasts may be key components of the bone metastasis niche and therefore a potential therapeutic target in breast cancer.

© 2014 The Authors. Published by Elsevier Inc. This is an open access article under the CC BY-NC-SA license (<http://creativecommons.org/licenses/by-nc-sa/3.0/>).

Abbreviations: BP, Bisphosphonate; ECM, Extracellular matrix; GFP, Green fluorescent protein; HSC, Hematopoietic stem cell; NBP, Nitrogen-containing bisphosphonate; PBS, Phosphate buffered saline; ROI, Region of interest; TRAP, Tartrate resistant alkaline phosphatase; PINP, Procollagen type 1N-terminal propeptide; ZOL, Zoledronic acid.

* Corresponding author at: Medical School, University of Sheffield, Beech Hill Road, S10 2RX, UK.

E-mail addresses: mhaider1@sheffield.ac.uk (M.-T. Haider), I.Holen@Sheffield.ac.uk (I. Holen), neil.dear@sahmri.com (T.N. Dear), k.hunter@sheffield.ac.uk (K. Hunter), hannah.brown@sheffield.ac.uk (H.K. Brown).

Introduction

The majority of cancer deaths are due to metastatic disease, and the lack of effective anti-metastatic therapies reflects our incomplete understanding of the underlying biology of tumour cell spread. Breast, prostate and lung cancers are amongst the most common malignancies with a preference to metastasise to the skeleton [1]. Treatment at this stage is palliative and often includes a bone-sparing anti-resorptive bisphosphonate (BP) [2], with zoledronic acid being the most potent [3]. In breast cancer, the dissemination of malignant cells to bone is thought to be an early event and tumour cells may reside in a dormant state within the bone for many years before developing into the

incurable secondary disease [4]. Elucidating the signals that maintain tumour cell dormancy, as well as the triggers for escape to a proliferative state, is currently one of the most intensely studied areas of cancer biology.

There is a general consensus that components of the bone marrow microenvironment make up a ‘bone metastasis niche’, responsible for regulating tumour cell homing, survival and dormancy. To what extent this overlaps with the hematopoietic stem cell niche, a specialised microenvironment that regulates hematopoietic stem cell (HSC) function, survival and quiescence, is not fully established [5–7]. The HSC niche is described to include an endosteal niche, of which the main cellular components are cells of the osteoblastic lineage [8]. In addition to regulating HSCs, it is proposed that the same niche may be creating a beneficial microenvironment for disseminated tumour cells in bone. Using *in vivo* model systems, Shiozawa *et al.* have shown that prostate cancer cells and HSCs reside within the same niche in the bone marrow [7] and that disseminated tumour cells can displace HSCs from the niche resulting in growth of metastatic colonies [9,10]. This suggests that components of the HSC niche, including osteoblastic cells, may be involved in tumour cell homing to bone. However, it remains to be established whether the osteoblast is a critical component of the metastatic niche, as well as the specific role of the tightly coupled osteoclast. In a breast cancer xenograft model, we have demonstrated that both osteoblast and osteoclast number/mm trabecular bone surface is significantly altered by breast tumour colonies at early and advanced stages of bone metastasis, indicating that both cell types may be intimately linked to tumour progression [11].

Therapeutic targeting of the bone microenvironment with anti-resorptive agents is standard of care for breast cancer patients with established cancer-induced bone disease [2]. Intriguing data from the AZURE trial demonstrated increased survival and reduced bone metastases when zoledronic acid is given in the adjuvant setting [12]. Several *in vivo* studies have also reported that inhibiting osteoclastic bone resorption with BPs early in the development of bone metastases reduces cancer-induced bone disease and may slow down disease progression. Preventive treatment with BPs (prior to tumour cell injection) is shown to be more effective at reducing tumour growth in bone when compared to therapeutic scheduling (initiated once bone metastases are established). For example, ibandronate treatment (10 µg/kg/day) of animals with established intrafemoral MDA-MB-231 tumours reduced progression of osteolytic lesions and metastases but did not eliminate tumour growth and larger lesions were unaffected [13]. In contrast, when treatment was initiated prior to cancer cell injection (day –3), formation of new osteolytic lesions and incidence of metastases were reduced. Alterations to the metastatic site before tumour cell arrival may thus impede tumour cell engraftment in bone, which could result in more pronounced anti-tumour effects. Another study suggesting that the reported anti-tumour effects of bisphosphonates are due to alterations of the bone microenvironment showed that preventive treatment with olpadronate (1.6 µmol/kg/day, 2 days before MDA-MB-231 tumour cell injection) significantly reduced new bone metastasis formation, while a therapeutic protocol (1.6 µmol/kg/day, day 28 to day 46) did not affect tumour growth in bone [14]. The authors suggest that the preventive schedule reduced tumour growth by inhibiting the release of tumour growth factors by osteoclastic bone resorption, an established mechanism for driving progression of cancer-induced bone disease.

Most studies investigating BP-induced anti-tumour effects did not investigate the consequences of inhibiting osteoclast activity on the tightly coupled osteoblasts. As both cell types are now suggested to be part of the metastatic niche, it is of great interest to determine how preventive scheduling of anti-resorptive agents modify osteoblasts, and the potential implications for subsequent tumour cell homing and colonisation. It is possible that development of bone metastases is also inhibited by BPs modifying the size and/or availability of the metastatic (osteoblastic) niche. The available data on the potential direct vs. indirect effects of bisphosphonates on osteoblasts is somewhat contradictory, with studies

reporting a reduction of osteoblast activity and survival *in vitro* and *in vivo* [15–18] while others have reported a beneficial effect of NBP treatment on osteoblast development, survival and growth [19–21].

We hypothesise that modification of the cellular components of the bone metastasis niche by zoledronic acid may affect the ability of tumour cells to initiate bone metastasis. Here we present the first *in vivo* study to assess the early (days 1–10) effects of a single, clinically relevant, dose of zoledronic acid on the bone microenvironment suggested to be part of the bone metastatic niche, osteoblasts and osteoclasts. In addition, we determined how these rapid, zoledronic acid-induced, changes to the bone microenvironment may affect early colonisation of particular areas of bone by breast cancer cells.

Materials and methods

Animal models and drug treatment

BALB/cAnNCrI *Foxn1^{nu/nu}* immunocompromised (athymic nude) mice were obtained from Charles River (Kent, UK). A transgene engineered to express GFP under the control of type 1 collagen promoter (pOBCol2.3GFPemd, kindly provided by Prof. David Rowe, University of Connecticut, USA) was introduced into the BALB/cAnNCrI nude mice by repeated backcrossing to generation N₅. Heterozygous nude mice were then intercrossed to generate homozygotes. This line (BALB/cAnNCrI.Cg-Tg(Col1a1-GFP)Row *Foxn1^{nu/nu}*) results in immunocompromised mice expressing GFPemd in cells of the osteoblast lineage and was used as a model to investigate the link between disseminated cancer cells and resident osteoblasts. Mice were housed in a controlled environment with a 12 h light/dark cycle at 22 °C. They were provided with *ad libitum* access 2018 Teklad Global 18% protein rodent diet containing 1.01% Calcium (Harlan Laboratories, UK) in individually ventilated cages (Tecniplast, Milan, Italy). All *in vivo* experiments complied with the UK Animals (Scientific Procedures) Act 1986 and were reviewed and approved by the local Research Ethics Committee of the University of Sheffield (Sheffield, UK). All work was performed under Home Office regulations (project licenses 40/3462 and 40/3531).

Cohorts of 6- and 12-week old female immunocompetent BALB/c or 6-week old immunocompromised BALB/c nude mice ($n = 2-7/\text{group}$) were used to assess the effect of zoledronic acid treatment on bone cells. To investigate the effects on osteoblasts in greater detail 6- and 10-week-old transgenic male mice ($n = 2/\text{group}$) expressing GFP-positive osteoblastic cells on a BALB/c nude background (described above) were used.

Animals were randomised into two treatment groups: (1) PBS and (2) zoledronic acid (ZOL, 100 µg/kg i.p.; supplied as disodium salt by Novartis; equivalent to the 4 mg infusion used in the treatment of cancer-induced bone disease) and sacrificed on days 0, 1, 3, 5 and 10 post injection (Fig. 1A). Hind legs were collected and fixed in either 10% buffered formalin prior to µCT analysis or 4% PFA solution before decalcification (0.5 M EDTA, 0.5% PFA, PBS, pH 8). Blood was collected and spun down at 4000 rpm for 10 min at 4 °C and serum was stored at –80 °C prior to analysis of serum bone turnover markers.

Bone metastasis model

To assess the effect of pre-treatment with ZOL on tumour cell homing to bone 8–13-week old female BALB/c mice (heterozygote or homozygote nude) with GFP expressing cells of the osteoblast lineage were injected with PBS or ZOL (100 µg/kg i.p.) on day 0. Animals were injected with 1×10^5 MDA-MB-231-NW1 (luc2 positive) breast cancer cells intracardiac and sacrificed on day ten (Fig. 1B). Immediately before injection, tumour cells were labelled with the lipophilic dye DID (Life Technologies, Paisley, UK) according to the manufacturer's instructions. Whole blood was collected, all samples from one treatment group were pooled, red blood cells were lysed, and the number of DID positive (DID+) tumour cells/mL was determined by flow cytometry. Bone

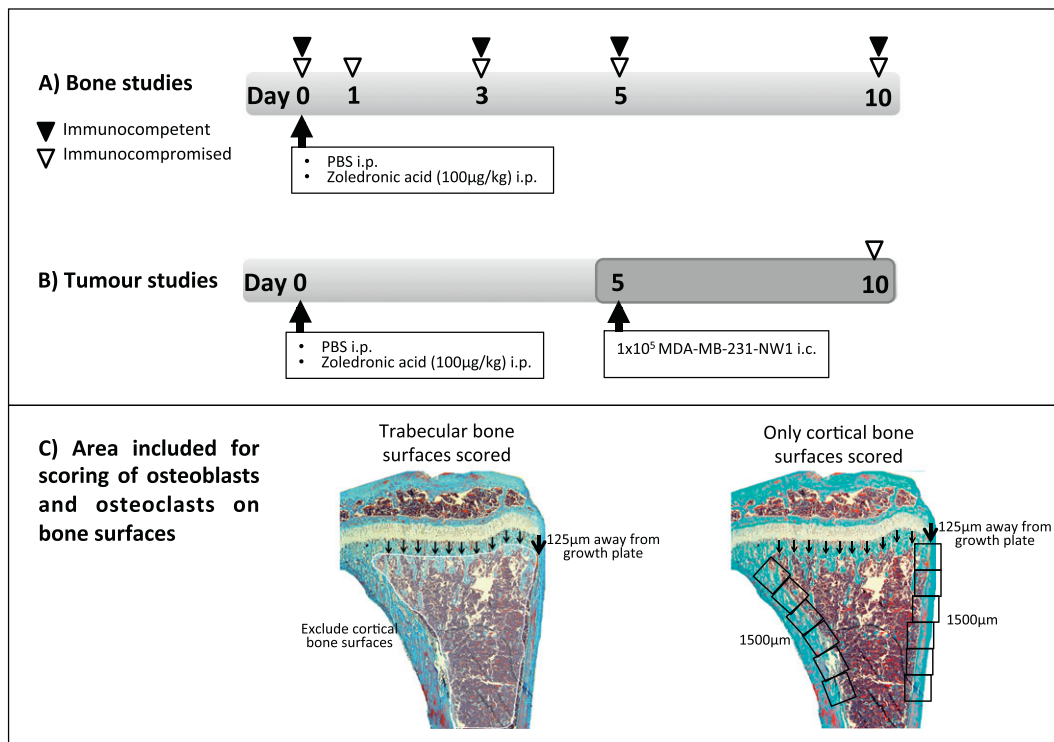


Fig. 1. *In vivo* studies, experimental outline. (A) Immunocompetent 6- or 12-week old balb/c ($n = 2-7$ /treatment group and time point) or immunocompromised 6-week old balb/c nude mice ($n = 3$ /day PBS, $n = 4$ /day ZOL) were injected intraperitoneally with a single dose of ZOL (100 µg/kg) or PBS on day 0 and sacrificed on the days indicated by white/black arrowheads. (B) Genetically engineered balb/c (heterozygote or homozygote nude) with GFP expressing cells of the osteoblast lineage received the same treatment and were injected with 1×10^5 MDA-MB-231-NW1 breast cancer cells i.c. on day 5 before sacrifice on day 10 ($n = 4$ /treatment group, 2 repeats). (C) Schematic description of the areas used for analysis of bone cells on trabecular and cortical surfaces.

marrow of femurs and tibias was flushed, pooled for all animals in each treatment group, red blood cells were lysed and the number of DID + tumour cells was determined by flow cytometry. To assess tumour cell growth, the remaining cell suspensions were plated into 6-well plates containing DMEM + GlutaMAX + Pyruvate supplemented with 10%FCS, 5% Pen Strep, 5% fungizone, and 1 mg/mL G418. In addition brain, liver, lung, spleen and kidneys were mechanically disrupted, passed through a 100 µm cell strainer and plated into 6-well plates. *Ex vivo* cultures were left to grow for 14 days and media were changed every 2 days before visualisation of bioluminescence using IVIS.

Multiphoton microscopy

Tibias were snap-frozen in liquid nitrogen and embedded into Cryo-M-Bed (Bright Instrument Co. Ltd, Huntingdon, UK). The growth plate was exposed using a Bright OTF Cryostat and a 3020 microtome (Bright Instrument Co. Ltd, Huntingdon, UK). A stack area of $2104 \mu\text{m} \times 2525 \mu\text{m}$ with $70 \mu\text{m}$ depth was captured with a Zeiss LSM510 NLO upright multiphoton/confocal microscope (Carl Zeiss Inl, Cambridge, UK). For detection of tumour cells in bone we visualised the DID-labelled cancer cells (DID + events) using a 633 nm laser. Because the size of the DID + events was variable we were unable to directly correlate the number of events with the number of tumour cells in bone. Bone matrix was visualised by second harmonic generation using a multiphoton laser at 900 nm (Coherent, Santa Clara, CA.). Quantification of DID + events within selected regions of interest was analysed using the Volocity 3D Image Analysis software 6.01 (PerkinElmer, Cambridge, UK).

Microcomputed tomography imaging

Microcomputed tomography analysis of proximal tibias and distal femurs was performed using a Skyscan 1172 X-ray computed

tomography (Skyscan) as reported previously [11]. Trabecular bone volume (BV/TV in %), number (Tb.N. in mm^{-1}) and cortical bone volume (mm^3) for tibias and femurs were calculated covering 1 mm, starting from the lowest part of the growth plate.

Osteoclast and osteoblast quantification

Osteoclasts and osteoblasts were quantified on histological sections following TRAP or H&E staining, respectively. TRAP staining of osteoclasts on histological sections ($3 \mu\text{m}$) and identification of osteoblasts using morphological criteria were done as previously described [11]. Osteoclast and osteoblast number/mm trabecular bone surface was then scored on two non-serial sections using a Leica RMRB upright microscope, a $10\times$ objective and OsteoMeasure software (Osteometrics). In order to determine bone cell number per mm/trabecular bone all trabecular surfaces $125 \mu\text{m}$ away from the growth plate were scored excluding the cortical bone surfaces. For cortical bone analysis scoring of osteoblasts lining the cortical surface was started $125 \mu\text{m}$ away from the growth plate and was performed for $1500 \mu\text{m}$ (Fig. 1C).

GFP immunohistochemistry

GFP expressing osteoblastic cells were identified by immunohistochemistry using an antibody specific to GFP. Dewaxed sections were incubated in 0.9% H_2O_2 for 10 min at ambient temperature prior to washing in dH_2O and PBS. Sections were transferred to 10% normal goat serum (Vector Laboratories, S1000) in PBS for 30 min followed by overnight incubation at 4°C with the primary antibody (anti-GFP rabbit IgG fraction polyclonal, Invitrogen, A11122, 1:600 in 5% normal goat serum). Slides were washed and incubated with the secondary antibody (goat anti-rabbit HRP, Insight Biotec, SC2004; 1:400 in PBS) for 45 min at ambient temperature. GFP was visualised using VECTOR NovaRED Peroxidase solution (Vector laboratories, Kit SK-4800).

Staining of growth plate cartilage

The metachromasia dye toluidine blue was used to stain acidic proteoglycan present in the growth plate of tibiae. Dewaxed and hydrated histological sections were immersed in toluidine blue working solution (Toluidine Blue O, Sigma Aldrich; 1% NaCl pH = 2.3) for 3 min at ambient temperature. Sections were then washed in dH₂O, dehydrated and cover slipped.

Osteoclast and osteoblast activity measured by ELISA

Osteoclast-derived tartrate-resistant acid phosphatase form 5b (TRACP 5b) in serum was measured using the MouseTRAP™ Assay (Immunodiagnostic Systems) and Rat/Mouse PINP Enzyme immunoassay for N-terminal propeptide of type I procollagen (PINP, Immunodiagnostic Systems) was used to determine osteoblast activity, both according to the manufacturer's instructions.

Statistical analysis

Statistical analysis was performed using Prism GraphPad (Version 5.0). Analysis was done by Student's *t*-test or two-way ANOVA and Bonferroni post-test. The applied test is indicated in each figure legend. A *p*-value of *p* < 0.05 was considered significant.

Results

A single dose of zoledronic acid induces early changes to bone volume and structure

In order to establish how quickly bone structure and volume were affected in young (6-week old) animals, we characterised the effects of a single dose of zoledronic acid (100 µg/kg, ZOL) or PBS 1, 3, 5 and 10 days post treatment by µCT analysis.

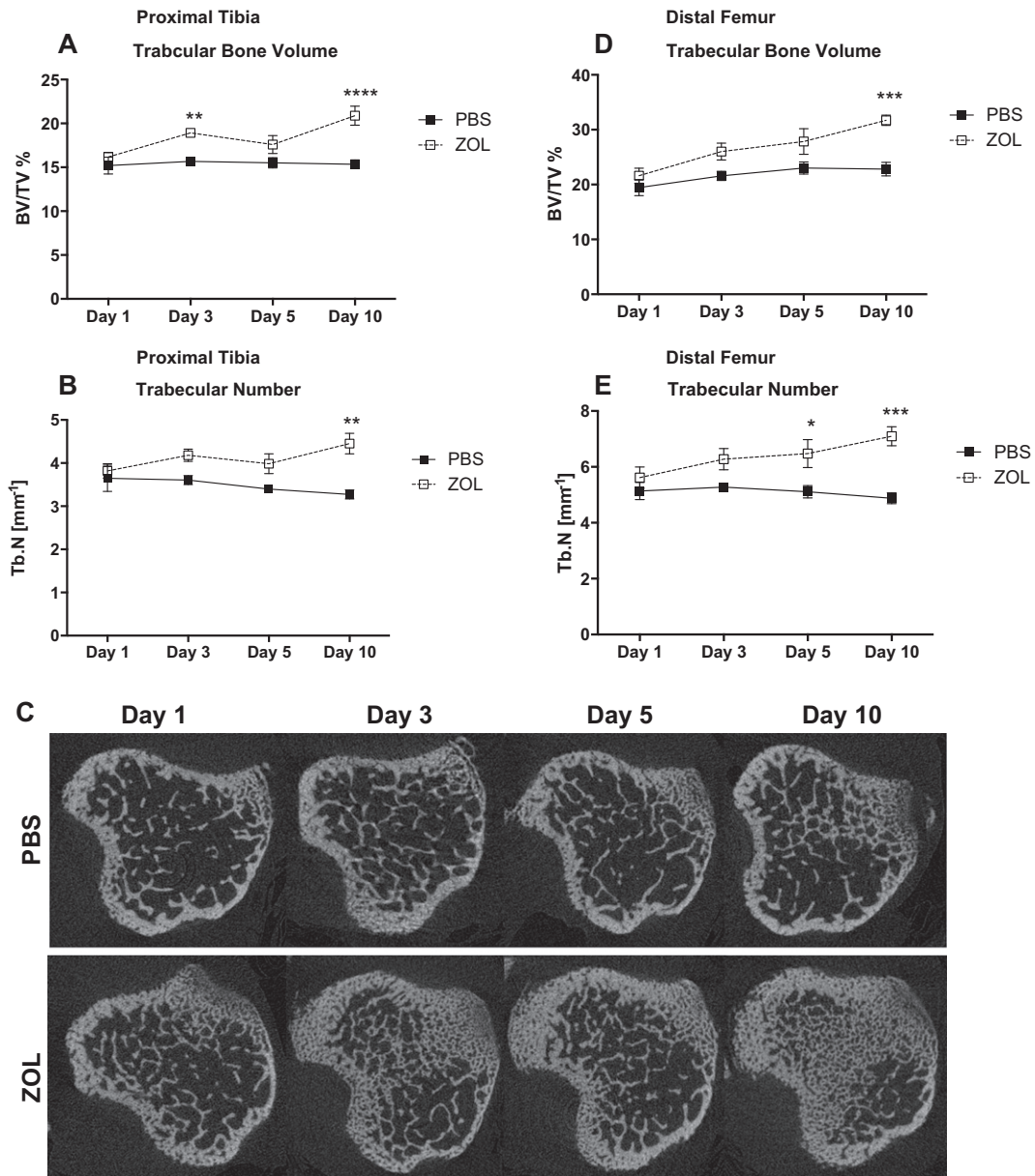


Fig. 2. Effects of a single dose of zoledronic acid on bone architecture. µCT analysis was performed to assess the immediate effects of a single dose of zoledronic acid (100 µg/kg, i.p.) on bone volume and architecture. Proximal tibia (A,B) and distal femur (D,E) were analysed for trabecular bone (A, D) expressed as % bone volume/tissue volume and trabecular number (B,E). Representative cross sections of tibiae are shown in (C). Two-way ANOVA and Bonferroni post-test: *****p* ≤ 0.0001, ****p* ≤ 0.001, ***p* ≤ 0.01. Day 1: *n* = 7, day 3: *n* = 7, day 5: *n* = 5 day 10: *n* = 5 for each time point and treatment group. All graphs show mean ± SEM.

ZOL caused a significant increase in trabecular bone volume of proximal tibias from day 3 onwards when compared to control animals (PBS: 15.67% vs. ZOL: 18.92%; $p \leq 0.01$; Fig. 2A). This increase was less prominent on day 5 but remained significantly elevated at day 10 (PBS: 15.35% vs. ZOL: 20.88%; $p \leq 0.0001$; Fig. 2A). ZOL also significantly increased trabecular number by day 10 (PBS: 3.27 mm^{-1} vs. ZOL: 4.45 mm^{-1} ; $p \leq 0.01$; Fig. 2B) when compared to PBS treatment. Representative cross sections of the proximal tibia illustrating this effect are shown in Fig. 2C.

Similarly, trabecular bone volume in the distal femur increased significantly compared to control 10 days after ZOL administration (PBS: 22.8% vs. ZOL: 31.72%; $p \leq 0.001$; Fig. 2D). Trabecular number was increased from day 5 up to 10 days post treatment (day 5: PBS: 5.11 mm^{-1} vs. ZOL: 6.47 mm^{-1} ; $p \leq 0.05$; day 10: PBS: 4.88 mm^{-1} vs. ZOL: 7.10 mm^{-1} ; $p \leq 0.001$; Fig. 2E).

These results clearly demonstrate that in young animals with high bone turnover, administration of a single, clinically relevant, dose of ZOL causes a rapid and significant increase in bone volume that is maintained for at least 10 days.

Zoledronic acid treatment induces rapid effects on bone cell activity and number/mm trabecular surface

We next established whether ZOL treatment also alters the number and activity of osteoblasts and osteoclasts, cell types suggested to be important for breast cancer progression in bone. For the analysis of osteoblast and osteoclast numbers per mm bone surface we focused on trabecular bone, as the majority of MDA-MB-231 tumours appear to originate in the trabeculae rich metaphysis area [11,22].

As early as three days after administration there was a significant reduction in osteoclast activity in ZOL treated animals compared to control, measured by serum TRAP concentration (PBS: 7.26 U/L vs. ZOL: 3.22 U/L; $p \leq 0.01$; Fig. 3A). This effect was transient and TRAP levels in the ZOL group started to increase again by day 5. The effect of the bisphosphonate on osteoclasts was further confirmed with the detection of a significant reduction in the osteoclast number on trabecular bone surfaces 3 days after ZOL injection compared to control (PBS: 4.97 vs. ZOL: 1.20; $p \leq 0.01$; Fig. 3C). The osteoclast number started to normalise to control levels on day 5. We also detected

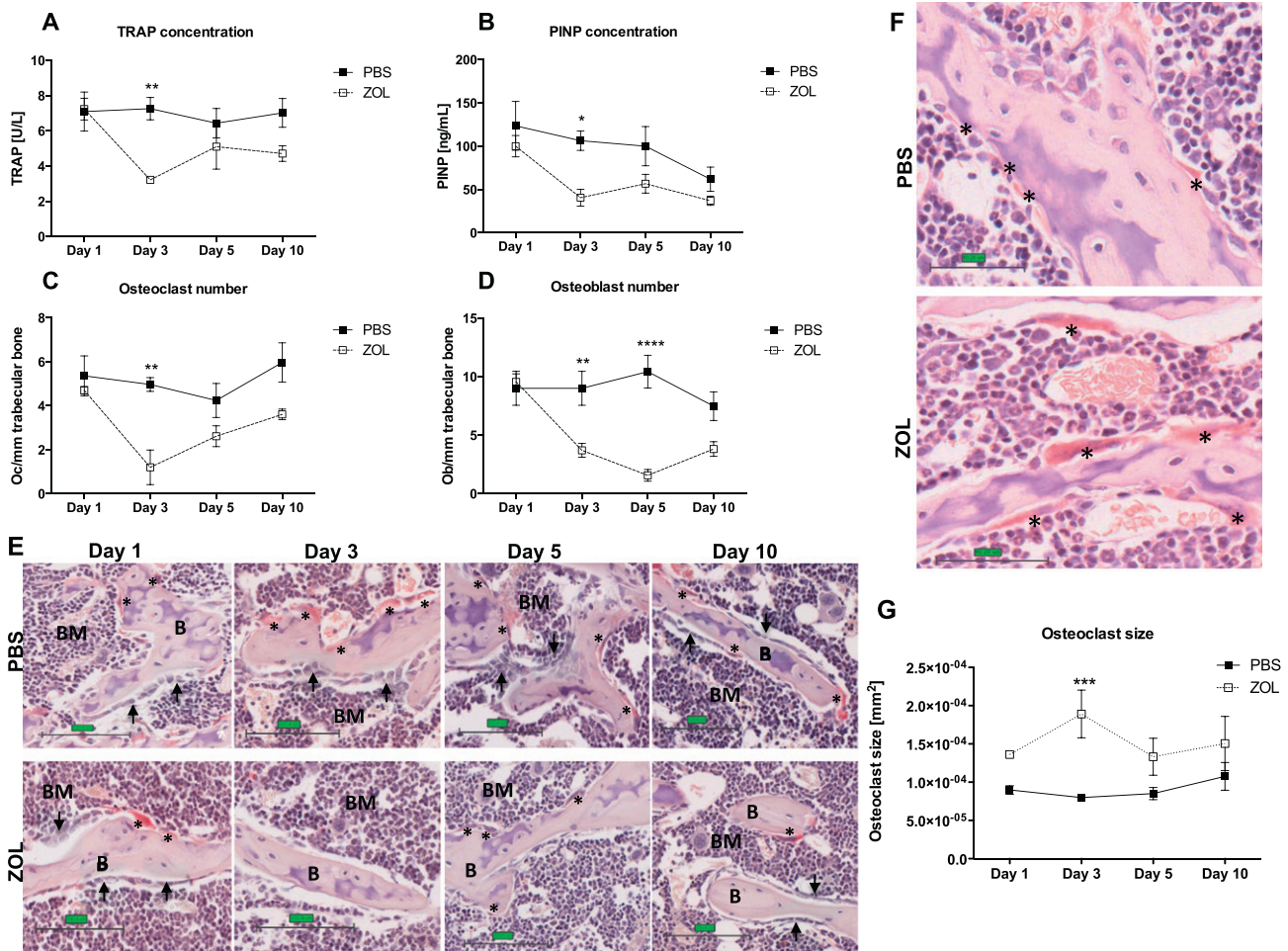


Fig. 3. Zoledronic acid-induced effects on osteoclasts and osteoblasts. (A) Tartrate-resistant alkaline phosphatase (TRAP) and (B) N-terminal propeptide of type I procollagen (PINP) concentration in serum samples of 6-week old female balb/c mice treated with a single dose of 100 $\mu\text{g}/\text{kg}$ ZOL or PBS were analysed 1, 3, 5 and 10 days after injection in order to determine osteoclast and osteoblast activity, respectively ($n = 5/\text{time point and treatment group}$). (C) Osteoclasts (Oc) per mm trabecular bone surface and (G) osteoclast size in mm^2 were scored on TRAP-stained histological sections. (D) Osteoblasts (Ob) per mm trabecular bone surface were scored on H&E stained sections of the right tibia. (E) Representative images of TRAP stained sections of proximal tibias. Scale bar = 100 μm , 20 \times magnification. Example images for osteoclast size difference post ZOL vs. PBS treatment are illustrated in (F). Scale bar = 50 μm . Arrows indicate rows of osteoblasts; stars indicate TRAP-positive osteoclasts (red). Day 1: $n = 7$, day 3: $n = 6$, day 5: $n = 7$, day 10: $n = 6$ for PBS and $n = 5$ for all time points for ZOL. Two-way ANOVA and Bonferroni post-test: **** $p \leq 0.0001$, *** $p \leq 0.001$, ** $p \leq 0.01$, * $p \leq 0.05$. All graphs show mean \pm SEM.

an increase in osteoclast size as early as 24 h after ZOL administration when compared to mice receiving PBS, which reached significance at day 3 (PBS: $7.99 \times 10^{-05} \text{ mm}^2$ vs. ZOL: $1.89 \times 10^{-04} \text{ mm}^2$, $p \leq 0.001$, Fig. 3F and G).

Osteoclasts were not the only bone cells affected by ZOL treatment. Osteoblast activity, measured by determining the serum levels of the bone formation marker PINP, decreased significantly 3 days post treatment in the ZOL group compared to control (PBS: 106.46 ng/mL vs. ZOL: 40.52 ng/mL; $p \leq 0.05$; Fig. 3B). Changes in the osteoblast number were in line with the PINP measurements; showing a sudden decrease in osteoblast number/mm trabecular bone in ZOL treated mice compared to control on day 3 (PBS: 9.00 vs. ZOL: 3.71; $p < 0.01$; Fig. 3D). Osteoblasts decreased further 5 days post treatment (PBS: 10.44 vs. ZOL: 1.56; $p \leq 0.0001$; Fig. 3D) followed by a slight increase on day 10. In a small subset of samples ($n = 4/\text{treatment group}$, day 5) we also analysed the number of osteoblasts/mm cortical bone, and found no significant reduction in osteoblasts on either medial or lateral bone surfaces when comparing the ZOL group to control mice (medial: PBS: 28.37 vs. ZOL: 22.71, $p = 0.4482$; lateral: PBS: 56.66 vs. ZOL: 45.81, 0.6101, data not shown).

These data show that the rapid ZOL-induced increase in bone volume is a result of effects on both osteoblasts and osteoclasts on trabecular bone surfaces.

Effects of a single dose of zoledronic acid on bone in immunocompromised mice

We repeated the experiment using immunocompromised animals required for xenograft models of breast cancer metastasis to bone. In agreement with the previous results, trabecular bone volume of tibias in the ZOL group was significantly increased on days 3 and 10 after treatment when compared to control (day 3: PBS: 7.21% vs. ZOL: 13.40%; $p \leq 0.01$; day 10: PBS: 11.24% vs. ZOL: 17.24%; $p \leq 0.05$; Fig. 4A). The trabecular number significantly increased as early as 3 days post ZOL treatment (day 3: PBS: 2.25 mm^{-1} vs. ZOL:

3.65 mm^{-1} ; $p \leq 0.05$; day 10: PBS: 2.49 mm^{-1} vs. ZOL: 4.81 mm^{-1} ; $p \leq 0.01$; Fig. 4B).

The effects of ZOL on osteoclast activity detected in immunocompetent animals were also confirmed, with a significant reduction in serum TRAP levels at 3 and 5 but not 10 days post ZOL injection when compared to control (day 3: PBS: 7.18 U/L vs. ZOL: 2.46 U/L $p \leq 0.001$; day 5: PBS: 5.70 U/L vs. ZOL: 1.97 U/L; $p \leq 0.01$; Fig. 4C). Furthermore, a reduction in osteoclast number per mm trabecular surface was observed from day 3 onwards (day 3: PBS: 7.30 vs. ZOL: 0.46 and day 5: PBS: 8.35 vs. ZOL: 0.88 both $p \leq 0.0001$; day 10: PBS: 7.05 vs. ZOL: 2.40, $p \leq 0.001$; Fig. 4D) which was mirrored by the bone formation serum marker PINP three days after treatment (PBS: 281.02 ng/mL vs. ZOL: 65.62 ng/mL, $p \leq 0.01$; Fig. 4E). In line with this, osteoblast number/mm bone surface decreased significantly from day 5 onwards in ZOL treated animals, compared to PBS (day 5: PBS: 14.73 vs. ZOL: 6.62; $p \leq 0.05$; day 10: PBS: 15.65 vs. ZOL: 5.66; $p \leq 0.01$; Fig. 4F).

The data show that the significant ZOL-induced changes in bone cell number and activity are independent of the immune status of the animals.

Visualisation of the zoledronic acid-induced osteoblast reduction in a mouse model with GFP-positive osteoblastic cells

For the quantification of osteoblasts, we identified the cells by assessing their specific morphology as previously described [11]. In addition, we used a model system where mice have been genetically engineered to express GFP in cells of the osteoblastic lineage, facilitating identification and visualisation of these cells. In these animals, the inhibitory effect of ZOL on osteoblastic cells was evident in tissues and histological sections (Fig. 5A) when compared to control. GFP staining visualised that ZOL treatment predominantly altered osteoblastic cells/mm bone surface in the trabecular bone area while the cell density around the growth plate and the cortical bone was unaffected (Fig. 5B). Toluidine blue staining showed that zoledronic acid appeared to increase the amount of proteoglycan rich matrix in the metaphysis, and this stretched deeper into the extending front of the growth plate compared

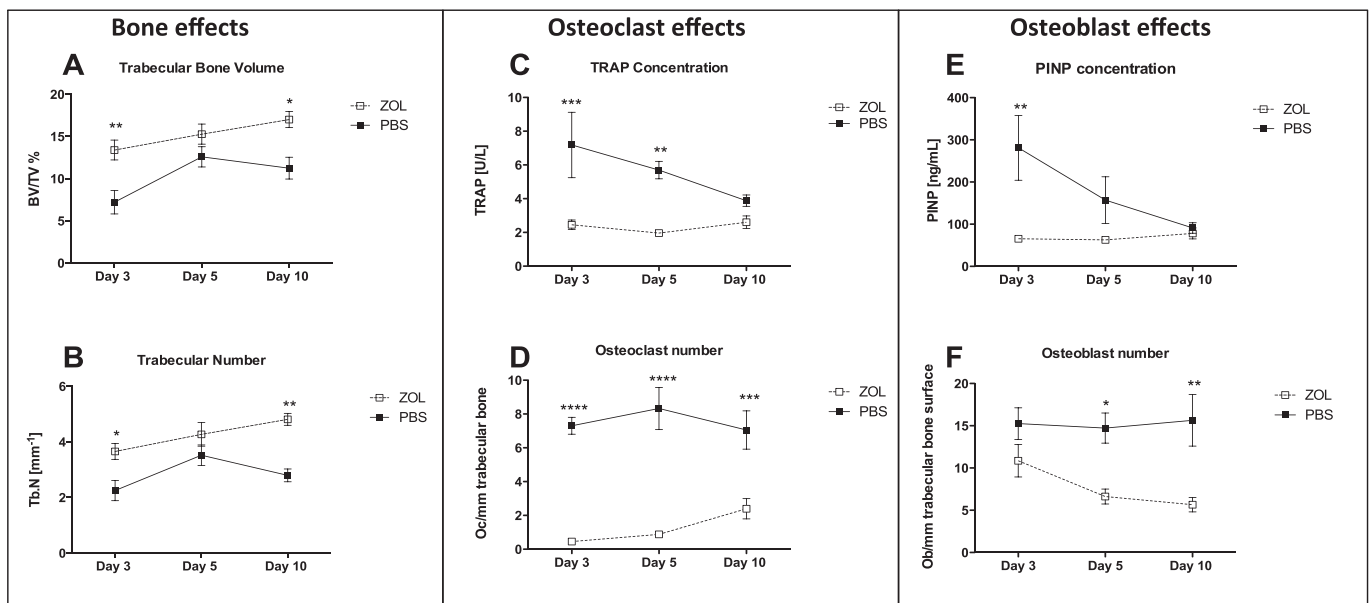


Fig. 4. Effects of ZOL treatment on bone and bone cells in immunocompromised mice. Female balb/c nude mice were injected with zoledronic acid (100 µg/kg, i.p.) or PBS to assess the effects of the drug on (A) trabecular bone volume, (B) trabecular number, (C) osteoclast activity measured in serum by TRAP ELISA, (D) osteoclast number per mm trabecular bone surface, (E) osteoblast activity measured in serum using PINP ELISA and (F) osteoblast number per mm trabecular bone surface. Animals were culled 3, 5 and 10 days post treatment. $n = 3/\text{day PBS}$ and $4/\text{day ZOL}$; for TRAP and PINP day 5: $n = 4/\text{group}$. Two-way ANOVA and Bonferroni post-test: **** $p \leq 0.0001$, *** $p \leq 0.001$, ** $p \leq 0.01$, * $p \leq 0.05$. All graphs show mean \pm SEM.

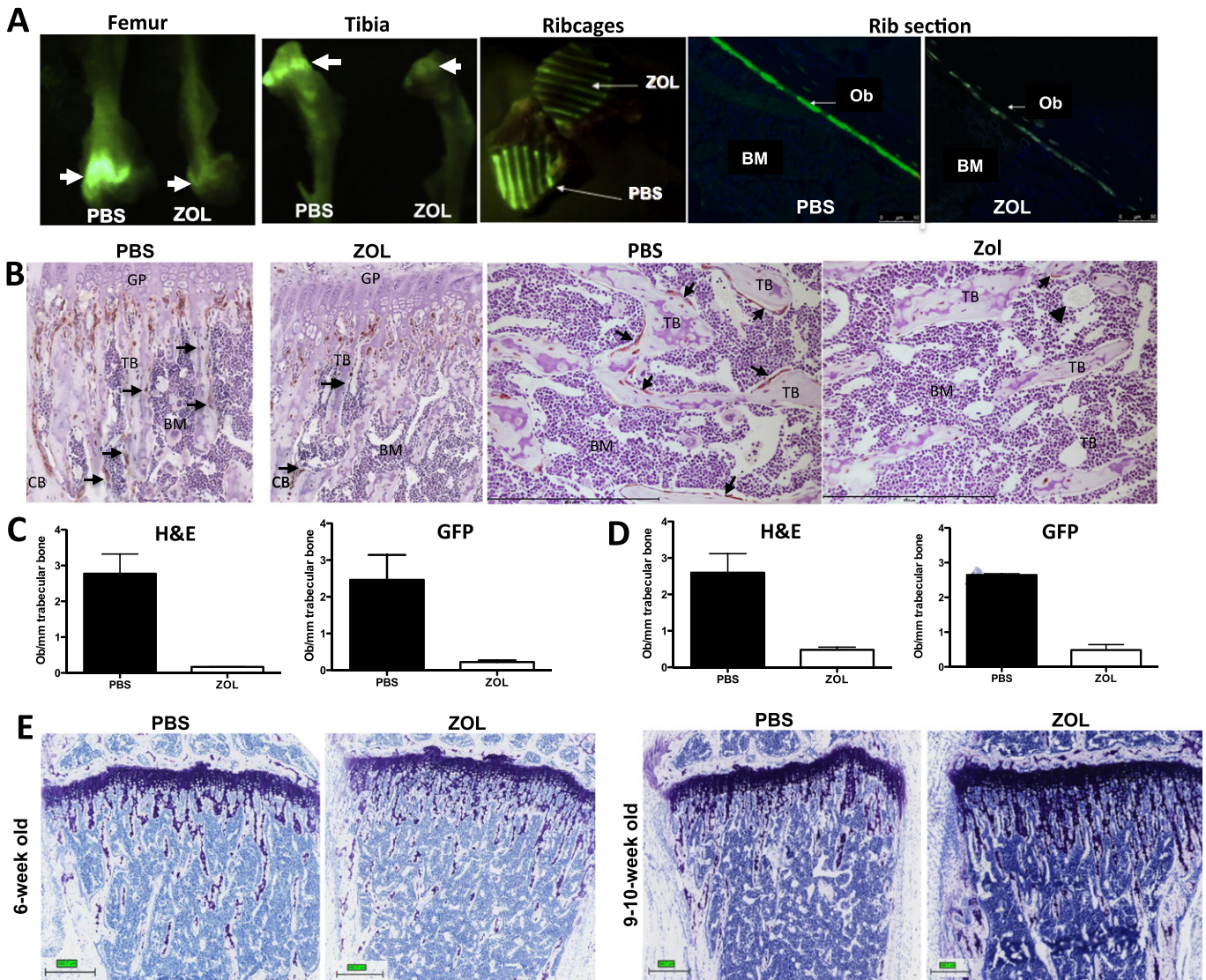


Fig. 5. Confirmation of ZOL-effects on GFP-expressing osteoblastic cells in a genetically engineered mouse model. (A) Reduction of GFP signal in tibia, femur, ribcages and rib sections of a ZOL treated mouse compared to control. Arrows indicate the osteoblast rich growth plate area. (B) The reduction in osteoblasts on trabeculi can also be seen by GFP-immunohistochemistry on paraffin sections of the tibia of 6-week old mice. Osteoblastic cells are stained brown, scale bar = 500 μm . Quantification of osteoblasts by morphology or after GFP-immunohistochemistry in (C) 6-week old mice ($n = 2/\text{group}$) and (D) 9–10-week old animals ($n = 2/\text{group}$) 5 days after a single injection of ZOL (100 $\mu\text{g}/\text{kg}$, i.p.) or PBS. Bottom panel (E) shows toluidine blue staining of proteoglycan in bone, scale bar = 300 μm .

to control mice (Fig. 5E). The ZOL-induced increase in bone volume may therefore be a result of elevated endochondral ossification, as this excess matrix is normally resorbed by osteoclasts.

In a small number of animals ($n = 2/\text{treatment group}$) we compared whether quantification of osteoblasts identified by morphology or GFP-immunohistochemistry results in comparable data sets. Both methods confirmed the reduction in osteoblasts on trabecular bone 5 days post ZOL injection when compared to control in 6 week-old mice (morphology on H&E: PBS: 2.77 vs. ZOL: 0.17; GFP-immunohistochemistry: PBS: 2.46 vs. ZOL: 0.22; Fig. 5C). Animals with a more mature skeleton and thus lower bone turnover (9–10 week-old, $n = 2/\text{group}$) also showed a reduction in osteoblast number/mm trabecular bone surface (morphology on H&E: PBS: 2.59 vs. ZOL: 0.48, GFP-immunohistochemistry: PBS: 2.65 vs. ZOL: 0.49 Fig. 5D).

Our data demonstrate a rapid ZOL-induced drop in osteoblasts/mm bone surface, accompanied by changes in the extra-cellular matrix of the growth plate that in combination may alter the composition of the bone metastasis niche.

Effects of zoledronic acid on tumour cell homing to bone

Next we investigated whether the significant ZOL-induced changes to the bone microenvironment would influence subsequent tumour cell homing to bone. Importantly, our experiments were carefully designed to ensure that tumour cell arrival coincided with the time point when the bone effects had reached their peak. In separate studies using the same model we have established that tumour cells home to bone within 24 h of intracardiac injection. Animals were pre-treated with a single dose of ZOL (100 $\mu\text{g}/\text{kg}$, i.p.) 5 days before intracardiac injection of DID-labelled tumour cells, and the presence of tumour cells in bone marrow, blood and a number of other organs was determined.

Analysis of two separate experiments ($n = 4/\text{treatment group}$ for each experiment) suggested a reduction in the number of tumour cells per millilitre blood in ZOL treated animals compared to those receiving PBS (Experiment 1: PBS: 163.27/mL vs. ZOL: 1.09/mL, Fig. 6A; Experiment 2: PBS: 290/mL vs. ZOL: 27.14/mL, Fig. 6C). To investigate whether ZOL treatment caused the tumour cells to localise to other (non-bone) sites we prepared *ex vivo* cultures of soft tissue cell

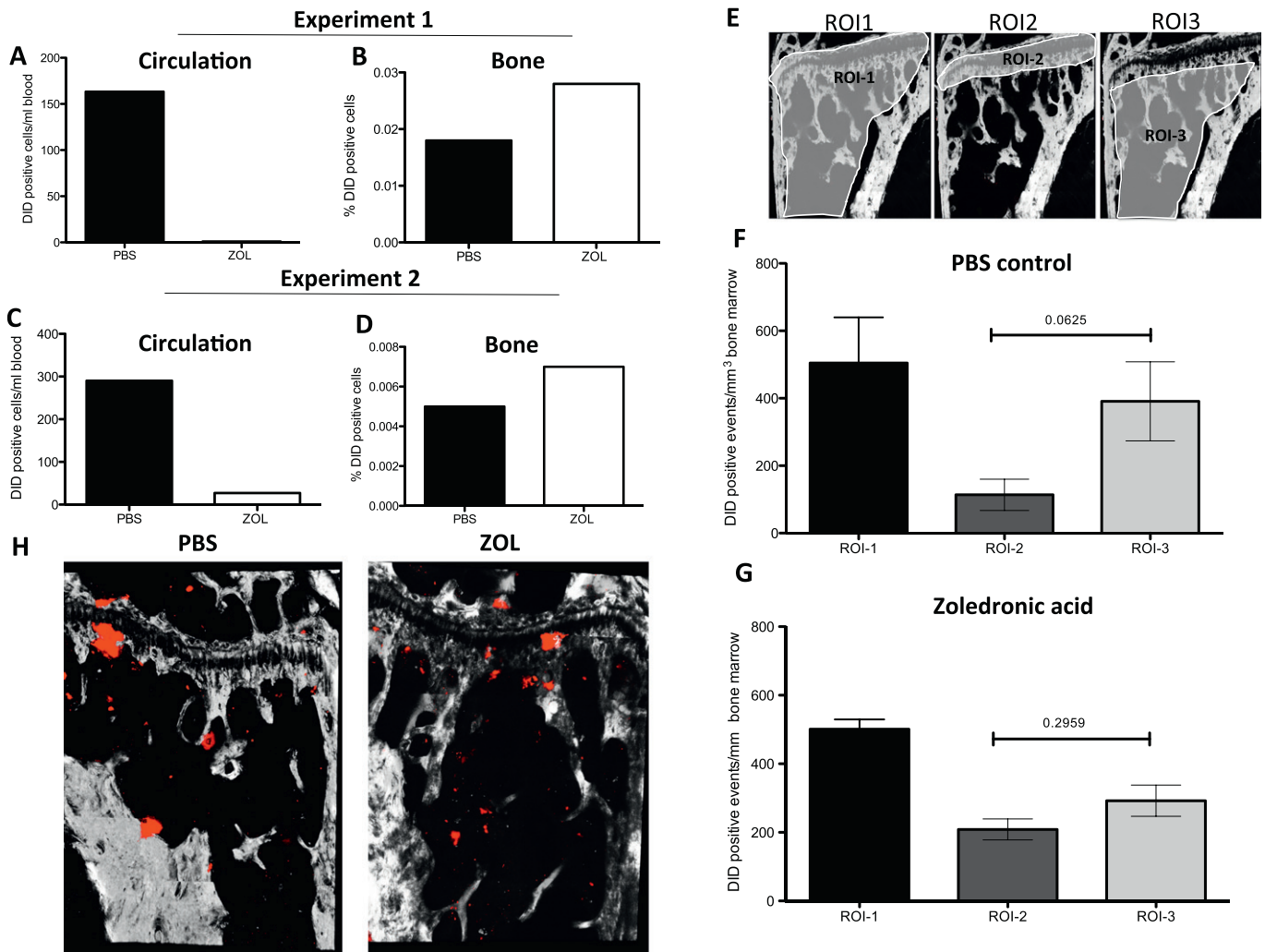


Fig. 6. Effects of ZOL-induced alterations to the bone microenvironment on tumour cell homing to bone. Two separate experiments ($n = 4$ /treatment group) were carried out to assess the effects of a single dose of ZOL (100 $\mu\text{g}/\text{kg}$) or PBS on tumour cell homing to bone (experiment outline Fig. 1B). Whole blood (A, C) and bone marrow (B, D) was collected, pooled for animals within one experiment for each treatment group and the number of DID + tumour cells assessed by flow cytometry. (E) Illustrates the regions of interest (ROI) used for analysis of tumour cells in bone by multiphoton analysis. The number of DID + events in each ROI is shown in (F) for PBS and in (G) for ZOL treated mice. Student's *t*-test, graphs show mean \pm SEM. (H) Representative multiphoton scans showing bone (white) and DID + events (red).

suspensions in one experiment and selected for MDA-MB-231-NW1 cells using antibiotic pressure *in vitro*. Tumour cells could only be detected in the lung culture of one out of four animals of the ZOL group. Pre-treatment with a single dose of ZOL did not greatly affect the percentage of tumour cells in bone when assessed by flow cytometry (PBS: 0.018% vs. ZOL: 0.028%, Fig. 6B; PBS: 0.005% vs. ZOL: 0.007%, Fig. 6D). Since we had shown earlier that ZOL administration predominantly affects osteoblastic cells/mm trabecular bone, but osteoblasts are still visible in the dense growth plate (Fig. 5B), we mapped the location of tumour cells to different areas in the bone using multiphoton microscopy. Three different regions of interest (ROI) were analysed including the growth plate (ROI-2), trabecular bone (ROI-3) and the total analysed area (ROI-1 = ROI-2 + ROI-3, Fig. 6E). Cortical bone was excluded and data from two separate experiments was combined for this analysis ($n = 6$ /treatment group). Comparison of tumour cells assessed by the total number of DID + events in ROI-1 showed no difference between PBS and ZOL treated mice (PBS: 504.68 vs. ZOL: 501.10, $p = 0.9799$, Figs. 6F and G), confirming the flow cytometry data. However, in control animals more DID + events were detected in the trabecular bone area (ROI-3) compared to the growth plate (ROI-2) (ROI-2: 113.65 vs. ROI-3: 391.03, $p = 0.0625$, Fig. 6F) although this did not reach statistical significance. In contrast, ZOL-induced

alteration of the bone before tumour cell injection appeared to blunt this preferential distribution (ROI-2: 208.67 vs. ROI-3: 292.44, $p = 0.2959$, Fig. 6G). Fig. 6H depicts representative multiphoton scans showing the bone structure as well as DID + events.

The data indicate that pre-treatment with the bisphosphonate reduced the number of circulating tumour cells, appeared to induce changes in the distribution of tumour cells within bone but did not affect overall number of tumour cells homing to bone. However, more independent experiments are required to validate these results.

Discussion

In this study we have established how a single, clinically relevant, dose of the anti-resorptive agent zoledronic acid modifies key cells of the bone microenvironment, suggested to be components of the metastatic niche. Although osteoclasts and osteoblasts have been shown to be part of the vicious cycle in late stage bone metastasis [23] it remains to be established whether these cell types also regulate cancer cell homing and/or trigger subsequent tumour cell proliferation. Bisphosphonates (BPS) are standard of care in the treatment of cancer-induced bone disease and are also proposed to exhibit direct and/or indirect anti-tumour effects *in vivo* [24,25]. Clinical trials of adjuvant

BPs in breast cancer have shown improved outcome in patients without bone metastases. A recent update of the AZURE trial showed that adjuvant treatment with ZOL, in addition to standard care in patients at high-risk of developing breast cancer bone metastasis, reduced the incidence of relapse in bone, demonstrating the beneficial effects of early ZOL treatment [12]. Although the underlying mechanisms remain to be established, these may include a reduction in the survival and/or progression of disseminated tumour cells in bone. This is supported by data obtained in model systems, showing that preventive regimens (i.e. administration of BPs prior to or at the time of tumour cell injection) appear more effective compared to therapeutic treatment of established tumours [24]. However, the focus of most preventive *in vivo* studies has been on reduction of tumour burden and the associated bone disease, without assessing the effects that alterations to the bone microenvironment may have for the subsequent tumour cell homing. In particular, the potential consequences of BP treatment on osteoblasts have not been investigated in this context. If osteoblasts are key components of the metastatic niche, BP-induced changes to their number and/or activity may in turn affect tumour cell homing to the niche. We have therefore characterised the early effects of a single, clinically relevant, dose of the potent BP zoledronic acid (ZOL) on osteoclasts and osteoblasts, both of which may be influencing tumour cell homing and progression. Importantly, we performed a detailed histomorphometric analysis of ZOL effects on trabecular bone in the tibial metaphysis, as this region is preferentially colonised by breast cancer cells in bone metastasis models [11,22].

Whereas long-term, repeated treatment with BPs is shown to result in a reduction of osteoclast activity [26–28] the acute effects of BPs on this cell type *in vivo* have not previously been described in much detail. Here we have shown that a single dose of ZOL inhibits bone resorption as early as 3 days after *in vivo* administration, demonstrating that repeated treatment cycles are not required for initiation of bone effects. The ZOL-induced changes to the osteoclasts were rapid and transient for some parameters, highlighting the importance of measuring both cell numbers and activity over time. The contradictory reports of ZOL effects on osteoclasts may be due to varying treatment schedules, model systems and the end points measured. However, it is generally accepted that repeated treatment with BPs inhibit osteoclast activity [26–28] and alter osteoclast morphology [29], resulting in increased bone volume. In agreement with this, we found a rapid increase in bone volume accompanied by a decrease in TRAP serum levels and increase in osteoclast size caused by a single administration of ZOL. The substantial effects of BPs on osteoclasts are commonly suggested to be the major mechanism of action behind their anti-tumour capacity [24]. However, ZOL has also been shown to exhibit significant anti-tumour effects in a model system using animals that lack functional osteoclasts, supporting that mechanisms other than reduction of osteoclastic bone resorption are involved in modifying tumour growth in bone [30].

Despite the close coupling between osteoclasts and osteoblasts, and their proposed role in the metastatic niche, few studies have investigated the effects of anti-resorptive agents on osteoblastic cells. We found a rapid ZOL-induced decrease in osteoblastic cells on trabecular bone surfaces, but were unable to establish whether this was due to a direct effect on the osteoblasts, or indirectly via osteoclast coupling. How BPs affect osteoblastic cells is not fully understood. Very low (nano- to pico-molar) concentrations of BPs are reported to cause increased osteoblast differentiation *in vitro* [20,21,31], and protect against glucocorticoid-induced apoptosis of osteoblasts and osteocytes both *in vitro* [32] and *in vivo* [33]. A number of *in vitro* studies have shown that long-term incubation of osteoblasts with high concentrations of BPs induced apoptosis and/or impaired proliferation [15–18]. However, the *in vivo* relevance of these studies is unclear. Due to the high bone affinity and rapid clearance of NBPs from the circulation, cells other than actively resorbing osteoclasts are only exposed to the drug for short times and at low concentrations following administration *in vivo*. A study by Idris et al. [17] reported that a single dose of

alendronate increased levels of unprenylated Rap1a in calvarial osteoblasts at 24 h, suggesting direct uptake of the BP *in vivo*. However, whether drug uptake was sufficient to affect cell activity/number was not determined. In support of our findings, osteoclast and osteoblast activity is shown to be significantly reduced compared to control after 3 weeks of ZOL treatment (0.05–1 mg/kg) *in vivo*, with a trend towards a decrease in cell number [34]. In addition, we have previously reported a significant reduction in osteoblast number 13 days after a single injection of 100 µg/kg ZOL *in vivo* [35]. Importantly, the rapid manifestation of the bone effects identified in the current study suggests that even a brief exposure to this potent agent may be sufficient to generate biological effects *in vivo*. Although we included a range of time points in this study including 1 and 3 days after treatment we could not find evidence of increased cell death after ZOL treatment in either TRAP stained sections or in sections with GFP positive osteoblastic cells.

In addition to identifying ZOL-induced effects on the number and activity of key bone cell types, we also found substantial changes in the matrix content of the growth plate. During bone development, pre-hypertrophic chondrocytes in the growth plate produce large amounts of extra-cellular matrix (mainly proteoglycan), which is followed by modelling and mineralisation by hypertrophic chondrocytes. At this stage the hypertrophic cells die, enabling the entry of cells of the ossification centre including osteoclasts, osteoblasts and endothelial cells [36]. BPs are reported to cause an elongation of the growth plate, suggesting that osteoclasts are required for the degradation of the cartilage matrix [37]. Interestingly, development of blood vessels precedes the invasion of osteoclasts around the chondro-osseous junction, which may facilitate extravasation of tumour cells to this area. We found that ZOL treatment appeared to result in accumulation of excess extracellular matrix resulting in a dramatic effect on the physical environment of the growth plate. This could affect the availability of soluble factors, as well as result in physical entrapment of tumour cells homing to this area. In ZOL treated animals, the remaining osteoblasts were predominantly located within the increased ECM of the growth plate, with potential consequences for the location of an osteoblastic niche.

The significant reduction in osteoclasts and osteoblastic cells, as well as the changes in extracellular matrix in the growth plate 3–5 days after ZOL administration, leads us to hypothesise that this could cause a modification of the metastatic niche and thus potentially influence tumour cell homing. Taking a novel approach to test this, we used multiphoton microscopy to quantify homing of tumour cells to different regions of the metaphysis, and assessed how this was modified by ZOL. When tumour cells were injected in animals where the putative niche area had been modified by pre-treatment with ZOL, their location and distribution appeared to be altered compared to that in control bones. We found a trend towards enrichment of tumour cells in the same region of the metaphysis where ZOL had induced accumulation of ECM, and where the majority of the osteoblasts were now located. This intriguing finding needs verification in independent studies, but may indicate that particular 'preferred' osteoblast-rich niche areas are present within the metaphysis. The mapping of tumour cells to specific areas of bone is technically challenging and it remains to be established how other elements influencing tumour cell homing to bone are modified by ZOL, including those of the vascular niche.

Despite inducing a trend towards altered tumour cell location, ZOL treatment did not reduce the total number of tumour cells in bone. The percentage of circulating tumour cells appeared dramatically reduced; however, the fate of circulating tumour cells after ZOL pre-treatment remains to be established and effects on tumour cell homing and growth in bone should be established using repeated dosing experiments.

The findings suggest that a single drug administration is not sufficient to prevent tumour development and progression. This is in agreement with results reported by Daubine et al. [38], investigating the effects of preventive ZOL dosing regimens on B02 breast tumour growth

in bone. Injection of a single dose of ZOL did not cause a significant change in tumour burden in bone on day 14, or reduce the area of osteolytic lesions or skeletal tumour burden present by day 32. Both daily and weekly regimens were beneficial for all these parameters, suggesting that repeated dosing with ZOL is required to prevent tumour progression in bone. In support of this, repeated treatment with ZOL is shown to increase elimination of disseminated breast cancer cells in breast cancer patients [39,40].

Conclusion

In summary, this study presents novel evidence that a single dose of zoledronic acid rapidly induces significant alterations to both the cellular component and the extra-cellular matrix of the metaphysis, the area of bone comprising the metastatic niche. Although total tumour cell number in bone was not altered there was a trend towards accumulation in osteoblast-rich areas after ZOL treatment. This is the first demonstration that breast cancer cells appear to preferentially localise to specific regions of the metaphysis, but that they may home to other areas if challenged by a modified microenvironment. Our data support that osteoblasts are a key component of the metastatic niche.

Source of funding source

This research was supported by Cancer Research UK (C13324/A11991), Breast Cancer Campaign (UK) (2010NovPhD17) and Yorkshire Cancer Research (S311).

Author's contributions

MTH carried out analysis of data, data presentation and participated in drafting and revising the manuscript. IH participated in study design, data interpretation, critical evaluation, revision and drafting of the manuscript. KH assessed histological sections, assisted with data interpretation and critically reviewed the manuscript for intellectual content. TND generated the pOBCol2.3GFPemd mice. HKB designed the study, performed experiments, interpreted data and participated in writing of the manuscript. All authors take responsibility for their work, have read and given final approval for publication of this manuscript.

Competing interests

The authors declare that they have no competing interests.

Acknowledgments

We thank Dr Wang N for his help with the multiphoton microscopy and transfection of the MDA-MB-231-NW1-luc2 cells, Mrs Evans CA for expert technical support and Dr Eaton C for his help with critical interpretation of data and as PPL holder. We thank Clare McCartney, Jan Bilton and Ben Woodman from the University of Leeds for assistance in mouse breeding. We also thank the PPL holder Prof Brown NJ.

References

- [1] Lipton A, Theriault RL, Hortobagyi GN, Simeone J, Knight RD, Mellars K, et al. Pamidronate prevents skeletal complications and is effective palliative treatment in women with breast carcinoma and osteolytic bone metastases: long term follow-up of two randomized, placebo-controlled trials. *Cancer* 2000;88(5):1082–90.
- [2] Coleman RE. Should bisphosphonates be the treatment of choice for metastatic bone disease? *Semin Oncol* 2001;28(4 Suppl. 11):35–41.
- [3] Widler L, Jaeggi KA, Glatt M, Muller K, Bachmann R, Bisping M, et al. Highly potent geminal bisphosphonates. From pamidronate disodium (Aredia) to zoledronic acid (Zometa). *J Med Chem* 2002;45(17):3721–38.
- [4] Riethmuller G, Klein CA. Early cancer cell dissemination and late metastatic relapse: clinical reflections and biological approaches to the dormancy problem in patients. *Semin Cancer Biol* 2001;11(4):307–11.
- [5] Guise T. Examining the metastatic niche: targeting the microenvironment. *Semin Oncol* 2010;37(Suppl. 2):S2–S14.
- [6] Psaila B, Lyden D. The metastatic niche: adapting the foreign soil. *Nat Rev Cancer* 2009;9(4):285–93.
- [7] Shiozawa Y, Havens AM, Pienta KJ, Taichman RS. The bone marrow niche: habitat to hematopoietic and mesenchymal stem cells, and unwitting host to molecular parasites. *Leukemia* 2008;22(5):941–50.
- [8] Calvi LM, Adams GB, Weibrecht KW, Weber JM, Olson DP, Knight MC, et al. Osteoblastic cells regulate the haematopoietic stem cell niche. *Nature* 2003;425(6960):841–6.
- [9] Shiozawa Y, Pedersen EA, Havens AM, Jung Y, Mishra A, Joseph J, et al. Human prostate cancer metastases target the hematopoietic stem cell niche to establish footholds in mouse bone marrow. *J Clin Invest* 2011;121(4):1298–312.
- [10] Shiozawa Y, Pienta KJ, Taichman RS. Hematopoietic stem cell niche is a potential therapeutic target for bone metastatic tumors. *Clin Cancer Res* 2011;17(17):5553–8.
- [11] Brown HK, Ottewill PD, Evans CA, Holen I. Location matters: osteoblast and osteoclast distribution is modified by the presence and proximity to breast cancer cells in vivo. *Clin Exp Metastasis* 2012;29(8):927–38.
- [12] Coleman RE, H. S., Bell R, Camreon D, Dodwell D, Liversedge V, Burkinshaw R, Keane M, Gil, M, Marshall H (2013). "Adjuvant therapy for stage II/III breast cancer with or without zoledronic acid. Final efficacy analysis of the AZURE trial." Cancer and Bone Society, Miami, Florida.
- [13] Neudert M, Fischer C, Krempien B, Baus F, Seibel MJ. Site-specific human breast cancer (MDA-MB-231) metastases in nude rats: model characterisation and in vivo effects of ibandronate on tumour growth. *Int J Cancer* 2003;107(3):468–77.
- [14] van der Pluijm G, Que I, Sijmons B, Buijs JT, Lowik CW, Wetterwald A, et al. Interference with the microenvironmental support impairs the de novo formation of bone metastases in vivo. *Cancer Res* 2005;65(17):7682–90.
- [15] Garcia-Moreno C, Serrano S, Nacher M, Farre M, Diez A, Marinosa ML, et al. Effect of alendronate on cultured normal human osteoblasts. *Bone* 1998;22(3):233–9.
- [16] Greiner S, Kadow-Romacker A, Lubberstedt M, Schmidmaier G, Wildemann B. The effect of zoledronic acid incorporated in a poly(D, L-lactide) implant coating on osteoblasts in vitro. *J Biomed Mater Res A* 2007;80(4):769–75.
- [17] Idris AI, Rojas J, Greig IR, Van't Hof RJ, Ralston SH. Aminobisphosphonates cause osteoblast apoptosis and inhibit bone nodule formation in vitro. *Calcif Tissue Int* 2008;82(3):191–201.
- [18] Orriss IR, Key ML, Colston KW, Arnett TR. Inhibition of osteoblast function in vitro by aminobisphosphonates. *J Cell Biochem* 2009;106(1):109–18.
- [19] Corrado A, Neve A, Maruotti N, Gaudio A, Marucci A, Cantatore FP. Dose-dependent metabolic effect of zoledronate on primary human osteoblastic cell cultures. *Clin Exp Rheumatol* 2010;28(6):873–9.
- [20] Fromiguet O, Body JJ. Bisphosphonates influence the proliferation and the maturation of normal human osteoblasts. *J Endocrinol Invest* 2002;25(6):539–46.
- [21] Xiong Y, Yang HJ, Feng J, Shi ZL, Wu LD. Effects of alendronate on the proliferation and osteogenic differentiation of MG-63 cells. *J Int Med Res* 2009;37(2):407–16.
- [22] Phadke PA, Mercer RR, Harms JF, Jia Y, Frost AR, Jewell JL, et al. Kinetics of metastatic breast cancer cell trafficking in bone. *Clin Cancer Res* 2006;12(5):1431–40.
- [23] Kakonen SM, Mundy GR. Mechanisms of osteolytic bone metastases in breast carcinoma. *Cancer* 2003;97(3 Suppl.):834–9.
- [24] Brown HK, Holen I. Anti-tumour effects of bisphosphonates—what have we learned from in vivo models? *Curr Cancer Drug Targets* 2009;9(7):807–23.
- [25] Holen I, Coleman RE. Anti-tumour activity of bisphosphonates in preclinical models of breast cancer. *Breast Cancer Res* 2010;12(6):214.
- [26] Dunford JE, Thompson K, Coxon FP, Luckman SP, Hahn FM, Poulter CD, et al. Structure-activity relationships for inhibition of farnesyl diphosphate synthase in vitro and inhibition of bone resorption in vivo by nitrogen-containing bisphosphonates. *J Pharmacol Exp Ther* 2001;296(2):235–42.
- [27] Roelofs AJ, Thompson K, Ebetino FH, Rogers MJ, Coxon FP. Bisphosphonates: molecular mechanisms of action and effects on bone cells, monocytes and macrophages. *Curr Pharm Des* 2010;16(27):2950–60.
- [28] van Beek E, Pieterman E, Cohen L, Lowik C, Papapoulos S. Farnesyl pyrophosphate synthase is the molecular target of nitrogen-containing bisphosphonates. *Biochem Biophys Res Commun* 1999;264(1):108–11.
- [29] Weinstein RS, Roberson PK, Manolagas SC. Giant osteoclast formation and long-term oral bisphosphonate therapy. *N Engl J Med* 2009;360(1):53–62.
- [30] Hirbe AC, Roelofs AJ, Floyd DH, Deng H, Becker SN, Lanigan LG, et al. The bisphosphonate zoledronic acid decreases tumor growth in bone in mice with defective osteoclasts. *Bone* 2009;44(5):908–16.
- [31] Koch FP, Merkel C, Al-Nawas B, Smeets R, Ziebart T, Walter C, et al. Zoledronate, ibandronate and clodronate enhance osteoblast differentiation in a dose dependent manner—a quantitative in vitro gene expression analysis of Dlx5, Runx2, OCN, MSX1 and MSX2. *J Craniomaxillofac Surg* 2011;39(8):562–9.
- [32] Plotkin LI, Weinstein RS, Parfitt AM, Roberson PK, Manolagas SC, Bellido T. Prevention of osteocyte and osteoblast apoptosis by bisphosphonates and calcitonin. *J Clin Invest* 1999;104(10):1363–74.
- [33] Plotkin LI, Bivi N, Bellido T. A bisphosphonate that does not affect osteoclasts prevents osteoblast and osteocyte apoptosis and the loss of bone strength induced by glucocorticoids in mice. *Bone* 2011;49(1):122–7.
- [34] Pozzi S, Vallet S, Mukherjee S, Cirstea D, Vaghela N, Santo L, et al. High-dose zoledronic acid impacts bone remodeling with effects on osteoblastic lineage and bone mechanical properties. *Clin Cancer Res* 2009;15(18):5829–39.
- [35] Brown HK, Ottewill PD, Evans CA, Coleman RE, Holen I. A single administration of combination therapy inhibits breast tumour progression in bone and modifies both osteoblasts and osteoclasts. *J Bone Oncol* 2012;1:47–56.

- [36] Mackie EJ, Tatarczuch L, Mirams M. The skeleton: a multi-functional complex organ: the growth plate chondrocyte and endochondral ossification. *J Endocrinol* 2011;211(2): 109–21.
- [37] Deckers MM, Van Beek ER, Van Der Pluijm G, Wetterwald A, Van Der Wee-Pals L, Cecchini MG, et al. Dissociation of angiogenesis and osteoclastogenesis during endochondral bone formation in neonatal mice. *J Bone Miner Res* 2002;17(6): 998–1007.
- [38] Daubine F, Le Gall C, Gasser J, Green J, Clezardin P. Antitumor effects of clinical dosing regimens of bisphosphonates in experimental breast cancer bone metastasis. *J Natl Cancer Inst* 2007;99(4):322–30.
- [39] Aft R, Naughton M, Trinkaus K, Watson M, Ylagan L, Chavez-MacGregor M, et al. Effect of zoledronic acid on disseminated tumour cells in women with locally advanced breast cancer: an open label, randomised, phase 2 trial. *Lancet Oncol* 2010;11(5):421–8.
- [40] Solomayer EF, Gebauer G, Hirnle P, Janni W, Luck HJ, Becker S, et al. Influence of zoledronic acid on disseminated tumor cells in primary breast cancer patients. *Ann Oncol* 2012;23(9):2271–7.